

# Ultrafast Optical Parametric Chirped-Pulse Amplification

Stefan Witte and Kjeld S. E. Eikema

(Invited Paper)

**Abstract**—In recent years, optical parametric chirped-pulse amplification (OPCPA) has emerged as a powerful tool for the generation of ultrashort pulses with extreme peak intensity. It has enabled the generation of phase-controlled few-cycle pulses in widely different parts of the spectrum. For the near-infrared spectral range, OPCPA is becoming an interesting alternative to conventional Ti:Sapphire-based laser technology for various applications. In this paper, we discuss the physics behind OPCPA, as well as the practical design considerations for the development of high-intensity, phase-stable few-cycle OPCPA systems. Also, we review the experimental achievements in ultrafast OPCPA systems to date.

**Index Terms**—Lasers, nonlinear optics, optical parametric chirped-pulse amplification (OPCPA), parametric processes, ultrafast optics, strong-field physics.

## I. INTRODUCTION

OPTICAL parametric amplification has been a well-known phenomenon since the early days of laser development [1], [2]. The increasing availability of high-intensity lasers has enabled the use of optical parametric amplifiers (OPAs) for a large number of applications, ranging from time-resolved studies to high-resolution spectroscopy. Especially, in the field of ultrafast science, OPAs are a powerful tool for the generation of ultrashort laser pulses with a high degree of flexibility, since large wavelength ranges can typically be covered with a single system. Progress in OPA technology has led to the generation of visible pulses with a duration as short as 4 fs [3], as well as the demonstration of few-cycle pulses in the infrared spectral range [4]–[7].

Typical OPA systems are normally optimized for either the shortest possible pulse duration, or for maximum wavelength tunability, and provide pulse energies in the microjoule to millijoule range [8]. While such OPAs are important tools for ultrafast spectroscopy, many experiments in strong-field physics require much higher light intensity. One of the most important concepts

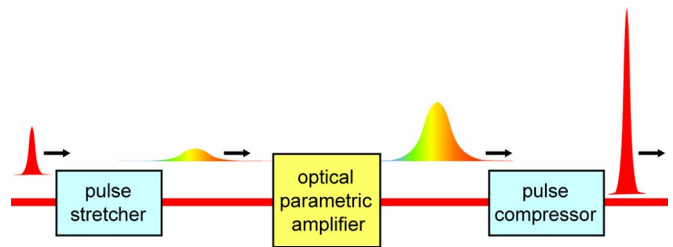


Fig. 1. Schematic principle of OPCPA.

for producing high-intensity, ultrashort laser pulses is known as chirped-pulse amplification (CPA) [9]. The invention of CPA advanced the development of Ti:Sapphire laser technology to the point, where the generation of multimillijoule, sub-50 fs pulses has become standard technology [10].

The integration of OPA and CPA into optical parametric chirped-pulse amplification (OPCPA, Fig. 1) combines the advantages of both techniques [11], [12]. It enables the production of high-intensity ultrafast laser pulses in various parts of the optical spectrum, with pulse durations in the few-cycle regime and peak powers reaching the terawatt (TW) level [13]–[15] and beyond. As a result of the phase-preserving properties of parametric amplification, OPCPA has enabled the production of intense carrier-envelope-phase-controlled few-cycle laser pulses in various parts of the spectrum.

It is clear that OPCPA is rapidly becoming an established technology in the field of ultrafast optics [16], [17]. In this paper, we review the various achievements so far in the field, with special emphasis on the use of OPCPA for generating few-cycle, phase-controlled pulses. We will describe the amplification of ultrabroadband spectra, the role of phase-matching, and the influence of parametric amplification on the phase of few-cycle pulses. Also, we discuss practical considerations that play a role in OPCPA design, and explore effects that are unique to high-energy ultrafast OPCPA systems.

## II. PRINCIPLES OF OPCPA

Optical parametric amplification is a three-wave-mixing process, which can be described by a set of coupled-wave equations (see, e.g., [6], [18], and [19])

$$\frac{\partial A_s}{\partial z} + \sum_{n=1}^{\infty} \frac{(-i)^{n-1}}{n!} k^{(n)} \frac{\partial^n A_s}{\partial t^n} = -i \frac{\chi^{(2)} \omega_s}{2n_s c} A_p A_i^* e^{-i\Delta \vec{k} \cdot \vec{z}} \quad (1a)$$

Manuscript received November 19, 2010; revised February 9, 2011; accepted February 15, 2011. The work of S. Witte was supported by the Netherlands Organization for Scientific Research under NWO Veni Grant 680-47-402. The work of K.S.E. Eikema was supported by the Netherlands Organization for Scientific Research under a NWO VICI Grant.

The authors are with the Institute for Lasers, Life and Biophotonics Amsterdam, VU University, 1081 HV Amsterdam, The Netherlands (e-mail: s.m.witte@vu.nl; k.s.e.eikema@vu.nl).

Color versions of one or more of the figures in this paper are available online at <http://ieeexplore.ieee.org>.

Digital Object Identifier 10.1109/JSTQE.2011.2118370

$$\frac{\partial A_i}{\partial z} + \sum_{n=1}^{\infty} \frac{(-i)^{n-1}}{n!} k^{(n)} \frac{\partial^n A_i}{\partial t^n} = -i \frac{\chi^{(2)} \omega_i}{2n_i c} A_p A_s^* e^{-i\Delta\vec{k}\cdot\vec{z}} \quad (1b)$$

$$\frac{\partial A_p}{\partial z} + \sum_{n=1}^{\infty} \frac{(-i)^{n-1}}{n!} k^{(n)} \frac{\partial^n A_p}{\partial t^n} = -i \frac{\chi^{(2)} \omega_p}{2n_p c} A_s A_i e^{i\Delta\vec{k}\cdot\vec{z}} \quad (1c)$$

where  $A_{s,i,p}$  are the complex pulse envelopes of the signal, idler, and pump fields, respectively. The  $k^{(n)}$ -terms are the  $n$ th-order dispersion coefficients of the medium,  $\chi^{(2)}$  is the second-order nonlinear susceptibility,  $n_{s,i,p}$  are the refractive indices of signal, idler, and pump, while  $\omega_{s,i,p}$  are their respective angular frequencies,  $c$  is the speed of light, and  $\Delta\vec{k}$  is the phase mismatch (which is discussed in detail in Section II-B).

There are three main components in these equations. The first term on the left-hand side describes the propagation (along the  $z$ -direction) in space of the different pulse envelopes. The second term on the left-hand side describes the dispersion of the different fields inside the nonlinear crystal, and contains a sum over all the dispersion orders. The term on the right-hand side is the nonlinear polarization, which contains the coupling between the different fields and is directly responsible for the parametric amplification process. Note that in the derivation of these equations, the slowly varying envelope approximation has been used.

When dispersion can be neglected, an exact analytical solution to (1) can be found in terms of Jacobi elliptic functions [18], [19]. A significantly simpler solution is obtained when pump depletion is assumed to be negligible (making this solution only valid in the initial stages of amplification)

$$I_s(z) = I_s(0) \cosh^2 gz \quad (2a)$$

$$I_i(z) = \frac{\omega_i}{\omega_s} I_s(0) \sinh^2 gz \quad (2b)$$

$$I_p(z) = I_p(0). \quad (2c)$$

The intensities  $I_{s,i,p}$  of signal, idler, and pump are related to the pulse envelopes  $A_{s,i,p}$  according to  $I_m = 1/2 \epsilon_0 c n_m |A_m|^2$ , where  $\epsilon_0$  is the vacuum permittivity. The parametric gain coefficient  $g$  is expressed as follows:

$$g = \sqrt{\chi^{(2)2} \frac{\omega_s \omega_i I_p(0)}{2\epsilon_0 n_s n_i n_p c^3} - \left(\frac{\Delta k}{2}\right)^2}. \quad (3)$$

When the gain is large ( $gz \gg 1$ ), the  $\cosh$  function in (2a) can be approximated as  $\cosh x \approx 1/2e^x$ , and consequently, the signal intensity becomes

$$I_s(z) \approx I_s(0) \frac{1}{4} e^{2gz}. \quad (4)$$

The small-signal gain is therefore found to depend exponentially on the pump intensity. From this last expression, we can estimate in the case of using a pump wavelength of 532 nm, a signal wavelength of 800 nm, and  $\beta$ -BaB<sub>2</sub>O<sub>4</sub> (BBO) as the nonlinear medium (having  $n = 1.65$  and  $\chi^{(2)} = 4 \times 10^{-12}$  m/V),

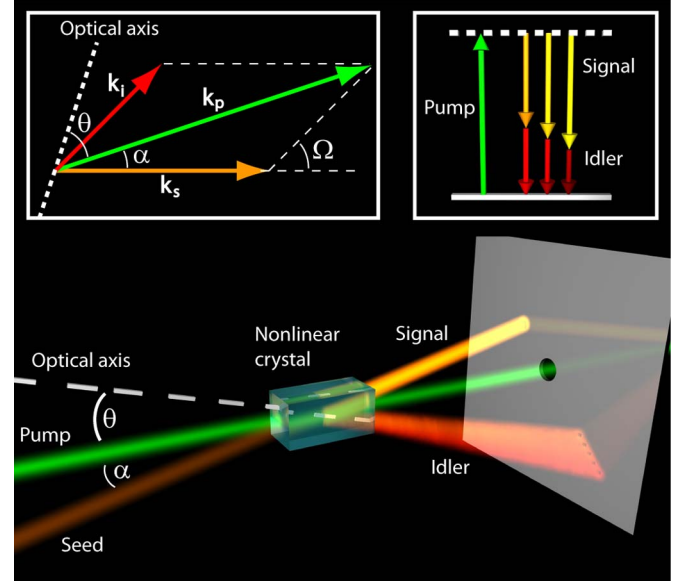


Fig. 2. Schematic of an OPA. The left inset shows the phase-matching geometry for noncollinear optical parametric amplification. The right inset shows the energy diagram for the parametric amplification process.

that a small-signal gain of  $10^4$  can be achieved in only 5 mm of material with a pump intensity of 4 GW/cm<sup>2</sup>.

#### A. Numerical Simulations

While the previous discussion provides basic insight into the physics of optical parametric amplification, a complete description of the behavior of a realistic OPCPA system requires that dispersion, pump depletion, etc., are properly taken into account. The common approach to OPCPA modeling is by numerically solving (1) with a split-step Fourier algorithm [20], [21]. The split-step approach is particularly suited for modeling pulse propagation in the presence of both nonlinearities and dispersion. The basic idea of the split-step algorithm is to divide the crystal into many small steps, and to calculate the nonlinear coupling terms and dispersion terms consecutively through each step. The nonlinear terms are then calculated in the time domain through numerical integration, while the dispersion is modeled in the frequency domain. This approach has the significant advantage that in the frequency domain, calculating the infinite sum in (1) reduces to multiplication with a single phase term.

Since the operators for the dispersion and nonlinear coupling are noncommuting, the split-step approach of calculating dispersion and nonlinearity in isolated, consecutive steps is not exact. However, it can be shown that the error decreases with  $h^2$ , where  $h$  is the step size through the crystal taken by the split-step algorithm. This scaling behavior ensures that the split-step algorithm rapidly converges for a sufficiently small step size.

A comprehensive analysis on the optimization of OPCPA systems was first given by Ross *et al.* [22]. More recently, several theoretical studies on ultrafast OPCPA have been performed [23]–[29], focusing on various aspects of OPCPA design, performance, and development.

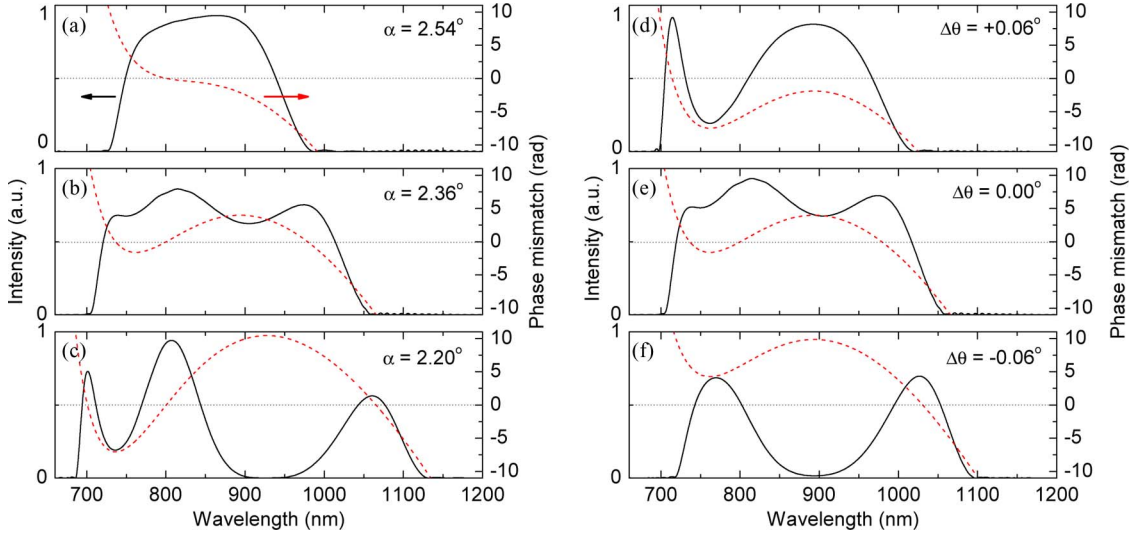


Fig. 3. Calculated gain spectra (solid) and spectral-phase mismatch (dashed) for noncollinear OPCPA in a 5-mm-long BBO crystal pumped at 532 nm (type-I phase matching). Panels (a), (b), and (c) show the effect of a change in the noncollinear angle  $\alpha$ , while panels (d), (e), and (f) show the spectral change resulting from tuning the phase-matching angle  $\theta$  around a value of  $\theta = 23.82^\circ$ . The wavelengths, where the phase mismatch is minimized correspond to regions of high gain.

### B. Phase Matching

The main parameter that governs the amplification process is the phase mismatch  $\Delta k$ , which can be written as follows:

$$\Delta k = k_p - k_s - k_i = \frac{n_p \omega_p}{c} - \frac{n_s \omega_s}{c} - \frac{n_i \omega_i}{c}. \quad (5)$$

Since  $\omega_p = \omega_s + \omega_i$  because of energy conservation, the phase-matching requirement places strict demands on the refractive indices of the respective beams inside the OPA crystal. While phase matching can typically be achieved by angle tuning of the crystal, dispersion will limit the spectral bandwidth over which phase matching is achieved. The phase mismatch can be expanded as a function of the signal frequency

$$\Delta k = \Delta k_0 + \frac{\partial \Delta k}{\partial \omega_s} \Delta \omega_s + \frac{1}{2} \frac{\partial^2 \Delta k}{\partial \omega_s^2} (\Delta \omega_s)^2 + \dots \quad (6)$$

To acquire a large phase-matching bandwidth, the first-order term  $\partial \Delta k / \partial \omega_s$  should be set to zero, while maintaining  $\Delta k_0 = 0$  as well [5], [30]. This requires an additional control parameter in the phase-matching process, for which the noncollinear angle  $\alpha$  between the pump and signal beams can be used [31], as illustrated in Fig. 2. It has been shown that the condition  $\partial \Delta k / \partial \omega_s = 0$  is essentially a statement of *group-velocity matching* [5], [30], [32]: this condition is fulfilled when the group velocities of signal and idler pulses are made equal along the seed beam propagation direction. Physically, fulfilling this condition ensures that the matching spectral components (i.e., those signal and idler frequency pairs that add up to the pump frequency, see the right inset in Fig. 2) of the signal and idler pulses remain overlapped over a long interaction length. This leads to a strong nonlinear conversion from pump to signal and idler, as can be seen directly from (1).

The influence of the phase mismatch on the gain bandwidth in OPCPA is demonstrated in Fig. 3, for the case of a 5-mm-long type-I BBO crystal pumped by 532 nm light. Panels 3(a)–(c)

show the influence of the noncollinear angle  $\alpha$ , while panels 3(d)–(f) demonstrate the effect of the phase-matching angle  $\theta$ . It can be seen that a change in  $\theta$  (around a value of to  $23.82^\circ$ ) gives a wavelength-independent vertical shift of the phase-mismatch curve, while a variation of  $\alpha$  leads to a tilt of the phase-mismatch curve (note that in the panels 3(a)–(c),  $\theta$  has been set for optimum phase matching at 800 nm). The gain is highest at points, where the phase matching is optimized, which leads to a three-peak spectrum for this particular OPCPA system. The ability to tune both  $\theta$  and  $\alpha$  provides a high degree of control over both central wavelength and width of the gain spectrum. For this particular phase-matching geometry, the gain spectrum suggests that a 7–8 fs pulse can be amplified. This has been confirmed experimentally [14], [33]–[36], and an amplified spectrum and its measured temporal pulse shape for a pulse with 2 TW peak power are shown in Fig. 4.

Instead of employing a noncollinear geometry, an alternative way of group-velocity matching is based on operating an OPA using type-I phase matching at degeneracy, i.e., in the spectral range, where signal and idler wavelengths are identical [7], [37]–[39]. In practice, a small noncollinear angle is still required in this type of setup, to be able to separate signal and idler beams (which have opposite chirp), and to prevent interference effects between them.

While in an ultrabroadband OPA, the group velocities of signal and idler are matched, the pump pulse will usually still have a different group velocity. Even when the group velocities of signal and idler are perfectly matched, this group-velocity mismatch (GVM) with the pump pulse can cause the signal and idler pulses to shift away from the pump pulse in time. Such a group-velocity walkoff can eventually limit the interaction length when the GVM-induced time delay becomes comparable to the pulse duration. While this GVM effect is a limiting factor in conventional ultrafast OPAs, the use of stretched pulses usually makes GVM negligible in OPCPA systems. Typically,

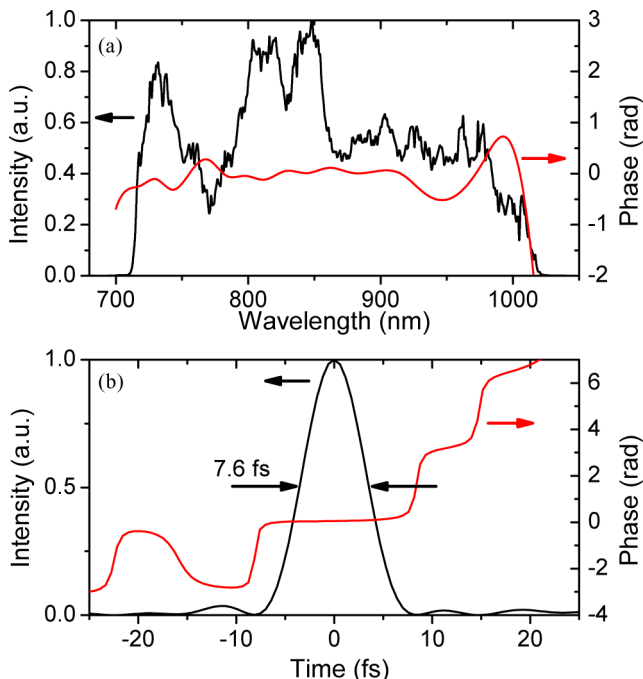


Fig. 4. Experimental results obtained with a three-stage BBO-OPCPA system pumped at 532 nm [34]. (a) Amplified spectrum and spectral phase after compression. (b) Corresponding pulse shape and phase in the time domain. The (FWHM) pulse duration is 7.6 fs, with an energy after compression of 15.5 mJ.

GVM effects become less important when the pulse duration exceeds the GVM-induced time delay by a factor of three or more [22].

### III. EXPERIMENTAL CONSIDERATIONS AND OPCPA DESIGN

In the design of high-power OPCPA systems, the use of a parametric process leads to significant differences compared to conventional laser-based amplifiers. Most of these differences originate from the instantaneous nature of the amplification process in OPCPA, as opposed to conventional laser amplifiers, where pump energy remains stored inside a crystal until it is extracted by the laser beam. As a result, there are several pitfalls when designing an OPCPA system by simply following the usual design routes for laser-based CPA systems.

An immediate consequence of the instantaneous amplification process is the need to match both the arrival times, and pulse durations of pump and seed pulses at the amplifier crystal. In addition, there are several more subtle effects resulting from the instantaneous parametric amplification process, which we will discuss in this section.

#### A. Pump-Seed Synchronization

The instantaneous nature of parametric amplification imposes significant requirements on the synchronization between pump and seed pulses. Not only do they need to arrive at the OPA crystals simultaneously, efficient amplification also requires the pulse durations of pump and seed to be in the same range. For few-cycle pulse amplification, the CPA stretching ratio is typically limited to  $10^3$ – $10^4$  to allow effective recompression

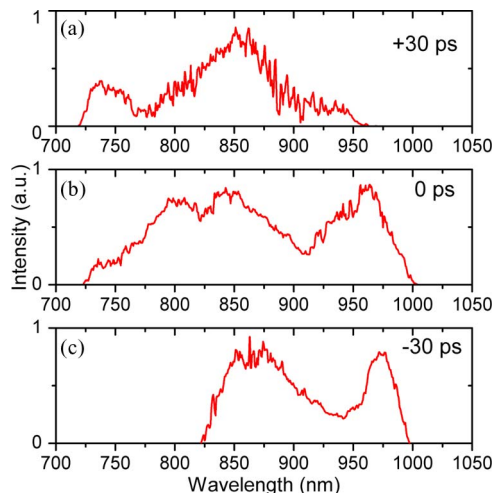


Fig. 5. Spectral changes resulting from a shift in pump-seed delay in an OPCPA system. Due to the chirp in the seed pulse, a change in arrival time between pump and seed pulses leads to a change in the amplified spectrum, as only a part of the seed spectrum overlaps with the peak of the pump pulse. A negative delay corresponds to the pump pulse preceding the seed. In this experiment, the pump pulse was 60 ps duration (Gaussian shape), while the seed pulse was 16 ps. The long-wavelength modulations in (a) are due to a double reflection of the seed in the BBO crystals, of which the leading (red) edge is amplified by the trailing edge of the pump pulse and spectrally interferes with the main pulse.

in view of higher order dispersion terms. In OPCPA, such a stretching ratio already suffices for amplification up to tens of millijoule energy with convenient few millimeter diameter beam sizes, and it is high enough for group-velocity walkoff effects [6] to be negligible. However, it also means that the pump pulse duration should be in the 10–100 ps range, much shorter than what is typically used for Ti:Sapphire pumping. Such powerful short-pulse lasers are much less widely commercially available than nanosecond duration pump lasers as used for Ti:Sapphire-based amplifiers, so that many groups have developed custom pump lasers for their OPCPA systems.

To achieve stable amplification, the pump and seed pulse arrival times at the OPA crystal should be synchronized to within a fraction of the pulse duration. For pulses with a 10–100 ps duration, this requires their relative timing to be stabilized with sub-ps accuracy.

Since the seed pulses are chirped, a change in the pump-seed timing can cause part of the seed spectrum to shift away from the peak of the pump pulse, leading to a spectrally dependent loss of gain. This is illustrated in Fig. 5, showing three experimental spectra recorded at different pump-seed delays. The pump and seed pulse durations are 60 and 16 ps, respectively. Because the seed pulse is positively chirped, a positive delay [i.e., pump arrives after seed, Fig. 5(a)] leads to selective amplification of shorter wavelengths, which are in the trailing edge of the seed pulse. For negative delays [pump precedes seed, Fig. 5(c)], the situation is reversed, and the longer wavelengths that are in the leading edge of the seed pulse experience the highest gain.

One approach to achieve the required sub-ps level of synchronization is by deriving both pump and seed pulses from a single laser source. This has been the common approach

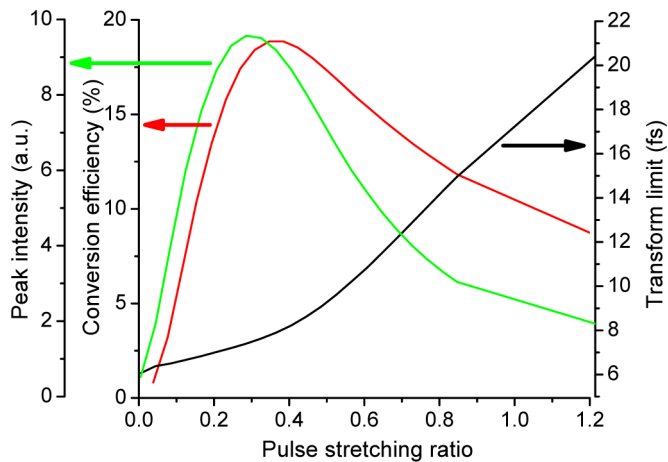


Fig. 6. Calculated Fourier-transform-limited pulse duration (black), pump-to-signal conversion efficiency (red), and achievable peak intensity (green) in an OPCPA system as a function of the seed-pulse duration, assuming Gaussian temporal pulse shapes for pump and seed. The pulse stretching ratio is defined as the duration of the chirped seed-pulse divided by the pump pulse duration. This simulation is performed for the specific case of a three-stage BBO OPCPA system (5 mm long crystals), pumped by 60 ps 532 nm pulses and seeded at 800 nm: note that the optimum stretching ratios can vary significantly depending on the amplification conditions (see text for details).

for OPAs [6], and can also be applied to OPCPA. The main limitation is that it requires a laser that emits both pump and seed wavelengths (or a subharmonic of these). This type of passive synchronization has been demonstrated using an ultrabroadband Ti:Sapphire oscillator to produce both a broadband seed at 800 nm and a pump pulse at 1053 nm [40]. Also, Ti:Sapphire pumped photonic crystal fibers have been used to produce optical solitons at 1064 nm, which can be used to seed a Nd:YAG pump laser [41].

Another way of synchronizing pump and seed pulses is through active electronic stabilization [33], [42], [43]. Through the use of high-frequency electronic feedback loops, the repetition frequencies of two separate mode-locked oscillators can be phase-locked with high timing stability. By controlling the phase between the repetition rate signals of the two lasers, the relative timing between pump and seed pulse can be changed electronically.

The passive timing stabilization has the advantage of being a compact, all-optical technique, but requires a single laser that can provide both pump and seed pulses with sufficient intensity and bandwidth. The active approach has the advantage that the pump and seed lasers can be individually chosen and optimized, and that only a small fraction of the light is needed for stabilization, but the electronic complexity of the system is increased compared to the passive stabilization method.

In OPCPA, the efficiency of the amplification process strongly depends on the ratio between the pump and seed pulse durations. Fig. 6 presents performance simulations of an OPCPA system as a function of the seed pulse stretching ratio, assuming a seed pulse with constant spectral bandwidth, and keeping the pump parameters fixed. While Fig. 6 only represents a specific OPCPA design rather than a general case, it does show an important issue in OPCPA, namely that the optimum energy extraction,

the shortest amplified pulse duration, and the highest obtainable peak intensity all require a different stretching ratio.

This can be explained in a straightforward way. If a seed pulse is much shorter than the pump, only a small part of the pump light will be utilized for amplification, resulting in a low efficiency. The amplified bandwidth will be broad in this case, as the entire seed spectrum overlaps with the peak of the pump pulse, leading to a short pulse duration. Stretching the seed pulse will initially provide a strong rise in efficiency, as the overlap with the pump pulse improves. However, as the seed pulse is stretched more, the edges of its spectrum shift away from the peak of the pump pulse and will experience a lower gain, resulting in spectral narrowing and a longer pulse duration. As the seed pulse is stretched to extend beyond the pump pulse duration, the efficiency may start to decrease again due to less effective seeding. This can easily be counteracted by increasing the pump intensity, although care should be taken to avoid increased levels of fluorescence. This complex interplay between stretching ratio, amplifier efficiency, spectral bandwidth, and effective fluorescence suppression is an important point of consideration in OPCPA design.

Clearly, the optimum stretching ratio depends on the design objectives. In general, there is a tradeoff between the optimal bandwidth–efficiency product and the achievable pulse duration. When optimizing peak intensity (which is equivalent to optimizing the bandwidth–efficiency product), a higher stretching ratio can be used, and it has been shown that increasing the stretching ratio between consecutive stages of an OPCPA system leads to a higher achievable peak intensity [25]. In this case, a stretching ratio around unity can be optimal in the final stage. However, when the objective is to produce the shortest possible pulse, a stretching ratio significantly below unity is required, since the entire seed bandwidth should be contained well within the pump pulse to achieve homogeneous amplification and make full use of the available phase-matching bandwidth.

Clearly, a rectangular shape for the pump pulse would be the optimal temporal profile for OPCPA, providing equal gain at any point in time and making optimal use of the available pump energy. Although making a square pulse with  $\sim 100$  ps duration is not straightforward, it has been experimentally realized for OPCPA pumping [44], [45].

A method known as time shearing provides a way to construct relatively efficient OPCPA systems with the use of nanosecond Nd:YAG pump lasers, which have the advantage that they are widely commercially available. The principle is to use multiple passes through the amplifier, each with a slightly different pump–seed delay [46]–[48]. In this way, the seed pulse depletes a different part of the pump pulse in every pass, thus using the available pump energy more efficiently, but at the cost of needing many more passes through the amplifier.

### B. Temporal Pulse Contrast

The pulse contrast, defined as the ratio between the pulse peak intensity and the intensity of the amplified parametric superfluorescence, is an important parameter for strong-field experiments. When focusing an ultrashort pulse to a small spot, the incompressible fluorescence background can easily reach an intensity

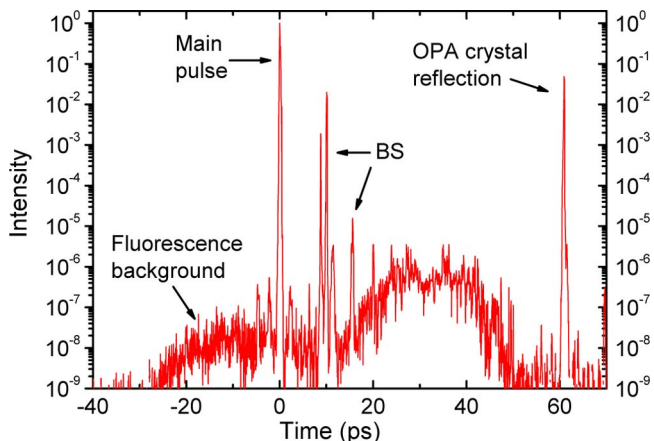


Fig. 7. Measured pulse contrast of a few-cycle multi-TW OPCPA system [34]. A fluorescence background with the duration of the pump pulse is visible, as well as some artefact peaks coming from multiple reflections in beamsplitters (BS) and one of the amplifier crystals. A prepulse contrast of  $2 \times 10^{-8}$  is obtained (see text for details).

level sufficient for ionization when the pulse contrast is low. The reported pulse contrast of different OPCPA systems varies widely: while some systems suffer from significant fluorescence background and are limited to a pulse contrast of  $10^{-4}$  [15], [49], other systems have been shown to achieve few-cycle pulses with a pulse contrast in the  $10^{-8}$  range [34], [50], [51]. An experimental contrast measurement is shown in Fig. 7, displaying the raw data for the measured pulse contrast of a 2 TW, 7.6 fs laser pulse. To extract the actual pulse contrast from such a measurement requires knowledge of the pulse broadening that occurs inside the measurement setup, as this will smear out the main pulse with respect to the background [34]. It is therefore also important that the entire spectral bandwidth of the pulse is used for the contrast measurement. After correction for the device-induced pulse broadening, the measured pulse contrast extracted from the data in Fig. 7 is found to be  $2 \times 10^{-8}$ .

The main ingredients for suppressing fluorescence and maintaining a high pulse contrast are the seed pulse intensity and the gain per amplification pass [34]. Since the generation of parametric superfluorescence is a process that competes with the amplification of the seed pulse, increasing the seed pulse intensity will improve the pulse contrast significantly. The temporal overlap between pump and seed pulses is also of influence, since an imperfect overlap will lead to the generation of fluorescence at those points in time, where there is no or only very little seed light available [25].

The gain per amplification pass is also an important parameter, as a high gain rapidly leads to significant amounts of superfluorescence. In typical experimental situations, where multiple amplification passes are used, any superfluorescence produced in the first pass can easily be amplified to high energy in subsequent passes. While a high single-pass gain does not necessarily lead to a low pulse contrast if sufficient seed intensity available, pump–seed matching becomes much more critical in this situation. Therefore, the use of multiple amplification stages with a lower gain per pass seems to be a more favorable approach for achieving a good pulse contrast.

A stable, low-noise pump laser is another important parameter in maintaining a high pulse contrast. It has been found that temporal modulations and random noise on the pump beam can translate into significant pedestals on the final compressed signal pulse [52]. The reason is that fast temporal modulations on the pump pulse will lead to rapid variations of the gain across the chirped seed pulse. This imprints high-frequency modulations on the amplified spectrum, which transform into a broad pedestal after pulse compression [53].

### C. Wavelength-Dependent Saturation Effects

Since the spectral components of the seed pulse are separated in time, they will not influence each other directly during an amplification pass. Each spectral component has its own “slice” of pump light available, and will be amplified depending on the pump intensity at that instance and the phase-matching conditions for that particular wavelength. As a result, each spectral component can experience a different regime of gain saturation, causing some spectral components to be deeply saturated, while others are still in the small-signal regime [24]. The shape of the amplified spectrum will therefore depend significantly on the amplification process, and a change in pump or seed intensity can cause a significant change in the spectral shape of the amplified pulse. As a consequence, also the temporal pulse shape and duration can change significantly upon saturation. An example of this effect is depicted in Fig. 8: as the saturation level increases, the spectrum around 800 nm saturates, and even experiences back conversion, while the intensity of the wavelengths near the edges of the spectrum still keep rising. Through this mechanism, pump intensity jitter can also lead to changes in the amplified spectrum, and affect the temporal shape of the amplified pulse.

A similar effect can be observed in the spatial domain, as spatially separated parts of the seed pulse will also amplify independently of each other. With a Gaussian-shaped pump beam profile, a situation can occur where the center of the beam experiences gain saturation, while the edges (where the pump intensity is lower) do not. This may lead to a spatially dependent amplified spectrum, and thus to a pulse duration that varies across the beam. The use of a pump beam with a flat-top spatial profile is therefore beneficial in OPCPA, as it ensures a constant gain across the entire seed beam. Upon saturation, the spatial profile of the amplified beam will start to adopt the shape of the pump beam, turning e.g., a Gaussian beam into a more flat-top profile. For pulses with a Gaussian beam profile, a graph similar to Fig. 6 can be drawn to show the dependence of the efficiency on the beam size ratio.

### D. Amplification of Few-Cycle Pulses

The ability to produce intense few-cycle laser pulses is one of the most attractive features of OPCPA. Aside from the required phase-matching bandwidth, the production of few-cycle pulses requires careful design of the CPA setup, since higher order dispersion terms become important in this regime. Dispersion management up to fourth- or even fifth-order is essential for pulse compression into the few-cycle regime. In this regard,

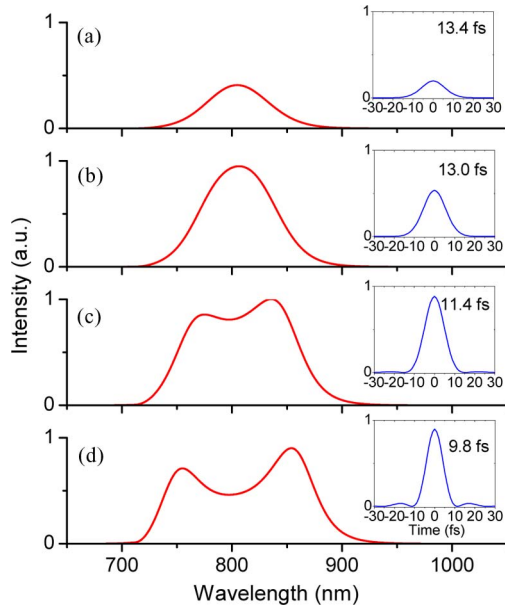


Fig. 8. Spectral changes resulting from gain saturation in OPCPA with a Gaussian temporal pump pulse shape. The seed intensity increases from top to bottom panel, as (a)  $I_s = 0.001$  GW/cm<sup>2</sup>, (b)  $I_s = 0.01$  GW/cm<sup>2</sup>, (c)  $I_s = 0.1$  GW/cm<sup>2</sup>, and (d)  $I_s = 0.5$  GW/cm<sup>2</sup>. The higher seed intensity leads to increased pump depletion, and therefore, gain saturation. Due to the chirp of the seed pulse, different spectral components experience a different gain, and can therefore be in a different saturation regime. This leads to significant reshaping of the signal spectrum. The insets show the Fourier-limited pulse shapes corresponding to each spectrum, which also show a significant change as a function of saturation.

OPCPA has some advantage over conventional laser systems, as only a small interaction length is required for substantial amplification. This minimizes the amount of material in the beam path, making it less problematic to match stretching and compression for multiple dispersion orders. Nevertheless, few-cycle pulse compression remains a challenge, and most groups therefore employ adaptive pulse compression techniques. By incorporating spectral phase-shaping devices, such as liquid-crystal spatial light modulators [14], [33], [34] or acousto-optic programmable dispersive filters [35], [38], [39], the total system dispersion can be minimized in a controlled way. Even with the use of adaptive compression, dispersion management remains an important issue in OPCPA design, as the compensation range of spectral phase-shaping devices is usually limited.

Various types of stretching and compression setups have been implemented in few-cycle OPCPA systems. Conventional grating-based CPA systems have been shown to work well [14], [33], [34], while also negative dispersion stretching and bulk material recompression has received significant attention [35], [38]. The latter approach has the advantage that the compressor losses are very low, but it does require more attention in keeping the seed pulse intensity sufficiently high to maintain an acceptable pulse contrast after amplification [39].

The choice of pump laser also influences the required stretching ratio. While many OPCPA systems are presently pumped by pulses with 50–100 ps duration, the use of shorter pump pulses significantly reduces the stretching ratio that is required for reaching significant conversion. Although this approach re-

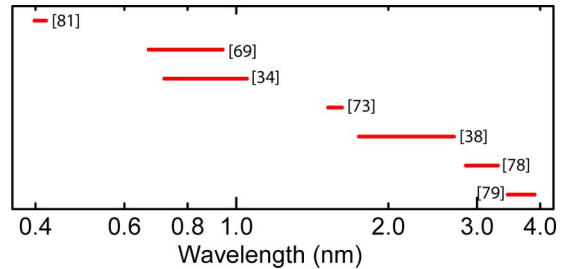


Fig. 9. Overview of the amplified bandwidths of various OPCPA systems that have been demonstrated in different parts of the spectrum. The respective references are given next to the spectral ranges.

quires an even more accurate pump–seed synchronization, it significantly relaxes the requirements for the CPA system, and also makes compensation of higher order dispersion terms less problematic. Intense pump pulses with 1–10 ps duration have already been demonstrated with Yb-based lasers [54]–[57].

Considering its properties, OPCPA seems naturally suited for few-cycle pulse generation, since the amount of material in the beam path is minimal, and the total path length from the seed oscillator to the final experiment can be kept as small as a few meters. One could say that in OPCPA, most of the system complexity is transferred to the pump laser, while the seed pulses are manipulated as little as possible. As few-cycle pulses are easily distorted by a small amount of dispersion or nonlinearity, such a “minimalist” approach is highly beneficial for generating ultrashort, high-intensity laser pulses.

#### IV. PHASE MATCHING AND WAVELENGTH FLEXIBILITY

One major advantage of parametric amplifiers is their wavelength flexibility, enabling the generation of powerful ultrashort pulses almost everywhere in the visible, near-IR, and mid-IR spectral ranges [6], [58] (see Fig. 9). By exploiting the different phase-matching conditions that can be obtained by using various crystals and pump wavelengths, the gain bandwidth of OPCPA can be optimized for a large range of seed wavelengths.

##### A. OPCPA Versus Ti:Sapphire

While Ti:Sapphire laser systems have been powerful workhorses for the ultrafast community [10], OPCPA systems have some interesting characteristics that make them a useful alternative to Ti:Sapphire in various cases. Especially, the combination of high-peak intensity and few-cycle pulse duration, where OPCPA can outperform Ti:Sapphire, is very useful for strong-field physics and ultrafast dynamics.

In the Ti:Sapphire wavelength range around 800 nm, the bandwidth for parametric amplification in BBO crystals is highly favorable. At a noncollinear angle of 2.3° (inside the crystal), the phase-matching conditions enable amplification of a 300-nm-wide bandwidth between ~720 and 1050 nm, when the OPA is pumped by 532 nm light (see Fig. 3). This full bandwidth can be used effectively for amplification, leading to ultrabroadband amplified spectra, with a corresponding Fourier-limited pulse duration in the 7–8 fs range, as shown in Fig. 4. Several experimental realizations have been reported on this type of OPCPA.

Notably, it has led to the first demonstration of sub-10 fs pulses with a peak intensity exceeding 1 TW [14], and multi-TW few-cycle pulses have been produced as well [15], [34], [36], [51].

The extension of OPCPA to extreme energy levels has been investigated using KD\*P crystals as the nonlinear medium, which has the advantage that it can be grown in large sizes. Pumped by the second harmonic of Nd:glass lasers at 527 nm, this approach has led to the generation of pulses with 35 J energy at 1050 nm [59]. Another system has been demonstrated by Lozhkarev *et al.* [60], [61], who achieved a peak power of 0.56 PW with 43 fs pulse duration, at 910 nm wavelength.

Instead of being a replacement, OPCPA systems have been used in combination with Ti:Sapphire, exploiting several of the advantageous features of each type of amplifier. This approach has led to various types of “hybrid” CPA systems [62], [63]. OPCPA systems have also been used as a front end in multi-TW to petawatt laser systems [64], [65] to provide a broadband seed pulse with a high temporal pulse contrast, which is an essential feature for strong-field experiments.

### B. OPCPA Throughout the Optical Spectrum

The ultrabroadband phase-matching bandwidth in non-collinear 400 nm pumped type-I BBO is well known from conventional OPA technology [4], [5], [30], [31], [66]–[68]. This geometry has been effectively exploited by Adachi *et al.* [69], [70], who also showed that shifting the pump wavelength to 450 nm can improve the phase matching even further. Using this approach, they generated 5.5 fs, 2.7 mJ pulses at 1 kHz repetition rate.

At wavelengths around 1500 nm, broadband amplification can be achieved using type-II phase matching in KTA crystals pumped by a Nd:YLF laser at 1053 nm, where 500  $\mu$ J, 130 fs pulses have been demonstrated [43], [71]. Recently, Mücke *et al.* showed that this approach can be scaled up significantly, producing 74 fs, 3.5 mJ pulses at 1.5  $\mu$ m, with 20 Hz repetition rate [72], [73]. This group used a four-stage OPCPA system with type-II KTP crystals, pumped by 1064 nm pulses. An interesting aspect this design is the additional generation of millijoule-level idler pulses at 3.5  $\mu$ m wavelength, which are not plagued by angular dispersion due to the collinear geometry. Periodically poled stoichiometric LiTaO<sub>3</sub> (PPSLT) has been demonstrated as an amplifier medium for 1500 nm when pumped by 1064 nm light [74], and for OPCPA seeded by a Cr:Forsterite laser at 1235 nm when pumped at 532 nm [75].

Phase-stable few-cycle pulse generation using OPCPA has been achieved at a wavelength of 2.1  $\mu$ m by Fuji *et al.* [38]. They used two periodically poled crystals (PPLN and PPLT) to amplify 20 fs pulses up to 80  $\mu$ J energy, at 1 kHz repetition rate. This approach benefits from a large phase-matching bandwidth by working at degeneracy. The output power was limited by the low seed energy available at 2.1  $\mu$ m, which was produced by intrapulse difference frequency mixing of an ultrabroadband Ti:Sapphire oscillator pulse. The use of a Ti:Sapphire amplifier improved the pulse energy to  $\sim$ 740  $\mu$ J, but a  $\sim$ 20% parametric superfluorescence background remained, leading to relatively high-pulse intensity fluctuations [76]. Nevertheless,

this approach to OPCPA has been shown to be feasible with low levels of superfluorescence [39]. Through minimization of the losses in the seed path, 200  $\mu$ J, 23 fs carrier-envelope phase (CEP) stable pulses at 2.2  $\mu$ m are generated with 1.5% rms energy stability.

Moving to even longer wavelengths in the mid-IR, phase-stable few-cycle pulses around 3  $\mu$ m wavelength have been produced by Chalus *et al.* [77], [78], who used PPLN crystals collinearly pumped by 1064 nm light. The signal pulse is produced through difference frequency mixing between two stable fiber amplifiers seeded by a single broadband fiber oscillator. This OPCPA system has been designed for high stability and a repetition rate of 100 kHz, producing up to 5  $\mu$ J pulse energy. Similar pulse parameters are obtained at an even longer wavelength of 3.4  $\mu$ m using MgO:PPLN crystals [79]. In this particular configuration, the use of aperiodically poled Mg:LiNbO<sub>3</sub> provides a significant improvement in phase-matching bandwidth [80].

On the short-wavelength side of the spectrum, OPCPA has been demonstrated to amplify 400 nm pulses by Wnuk *et al.* [81]. They employed type-I BBO pumped by the fourth harmonic of a Nd:YAG laser at 266 nm to produce 24 fs, 30  $\mu$ J pulses at 10 Hz repetition rate.

### C. Extending the Phase-Matching Bandwidth

While the standard approach to phase-matching involves tuning the crystal angle and the noncollinear angle between pump and seed beam, more ways to control the phase-matching bandwidth in OPCPA have been explored. One method to extend the phase-matching bandwidth even further is through the use of an angularly dispersed signal beam [82]–[84]. Mathematically, this comes down to minimizing also the second-order term in (6) [85]. While this approach seems promising for extending the phase-matching bandwidth, recollimation of an ultrabroadband angularly dispersed signal pulse is challenging experimentally.

Another possibility for improved phase matching is through angle or wavelength multiplexing of the pump beam. The use of two pump beams with slightly different angles provides phase matching at different signal wavelengths, thereby broadening the total phase-matching bandwidth [86], [87]. A similar broadening of the phase-matching bandwidth can be achieved by using a broadband pump pulse, as the various spectral components, each produce a slightly shifted phase-matching bandwidth. Combining this feature with angular dispersion of the pump beam can improve the phase-matching bandwidth significantly, and has led to the production of sub-4 fs pulses in a visible OPA [68]. The extension of this method to OPCPA has also been demonstrated experimentally [88]. Alternatively, the broadband pump pulse can be stretched in time, and the seed chirp adjusted in such a way that phase matching is achieved over a large seed bandwidth, while maintaining a collinear geometry [22], [89].

The use of two pump beams with a large wavelength difference provides another way to improve the phase-matching bandwidth. This was demonstrated by Herrmann *et al.* [90], who used the second and third harmonic of Nd:YAG to pump

consecutive BBO-OPCPA stages, achieving an amplified bandwidth that spans from 600 to 1050 nm.

### V. CEP CONTROL

For pulses in the few-cycle regime, the CEP is an important factor. Since parametric amplification preserves the phase of the signal beam, OPCPA can be expected to function as a phase-stable amplifier as well. The phase-preserving properties of OPAs have been confirmed experimentally [91], and have even been exploited to produce passively CEP-stabilized pulses [92] by using pump and signal pulses with the same phase, which leads to an idler pulse with a constant CEP. The phase stability of OPCPA systems has indeed been demonstrated [33], [93], and even phase-stable amplification to intensities exceeding 1 TW has been achieved [94]. Since intrapulse difference-frequency mixing has proven to be a convenient way of producing CEP-stable IR seed pulses, various CEP-stable OPCPA systems have been based on this principle [38], [39], [77].

It is important to realize, however, that the preservation of the signal phase during parametric amplification is an approximation, which is only valid for negligible pump depletion and/or perfect phase matching. This was already pointed out by Ross *et al.* [22]. By explicitly analyzing the phase components of the coupled wave (1), an expression for the signal phase after amplification can be found

$$\varphi_s(L) = \varphi_s(0) - \frac{\Delta k}{2} \int_0^L \frac{f}{f + \gamma_s^2} dz \quad (7)$$

where  $L$  is the crystal length,  $f = 1 - I_p(z)/I_p(0)$  is the fractional pump depletion, and  $\gamma_s^2 = \omega_p I_s(0)/\omega_s I_p(0)$ . This equation shows a dependence of the phase of the amplified signal beam on the pump intensity, for spectral components that have a nonzero-phase mismatch  $\Delta k$ . It is interesting to note that while the pump intensity is a significant factor, the phase of the pump beam does not have any influence on the phase of the amplified signal beam.

Since many OPCPA systems work in a regime of significant pump depletion to optimize efficiency, (7) states that there will be a coupling between the signal phase and the pump intensity. As a result, pump intensity fluctuations may introduce phase jitter on the amplified pulses. Note that the sign of this coupling depends on the sign of the phase mismatch  $\Delta k$ , which is wavelength dependent. This intensity-to-phase coupling has been investigated experimentally by Renault *et al.* [94], who also observed the  $\Delta k$ -dependence of the coupling. However, the main conclusion of this work was that excellent phase stability ( $< 1/25$ th of an optical cycle) can be achieved in OPCPA with an experimentally very reasonable pump intensity jitter of a few percent. The relative jitter between consecutive pulses in a double-pulse OPCPA system has also been measured [95], and is found to be sufficiently stable for various phase-sensitive experiments.

The effect of (7) is schematically depicted in Fig. 10. Fig. 10(a) shows the evolution of the integrand from (7) as a function of the interaction length  $z$ , for two different pump intensities that differ by 5%. The shaded area between these

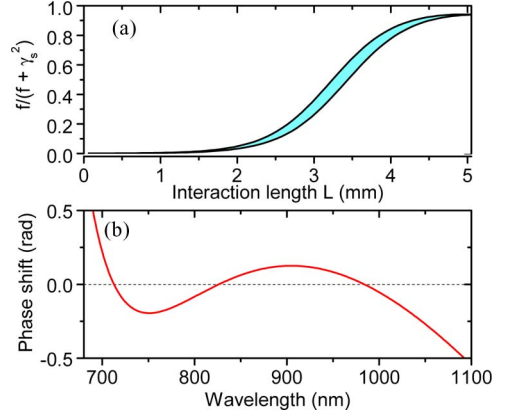


Fig. 10. (a) Argument of (7) in a saturated OPCPA stage at 800 nm, for the phase-matching conditions shown in Fig. 3(b). The two black curves correspond to a 5% difference in pump intensity. The colored area between the curves illustrates the difference, which gives rise to an intensity-dependent phase shift. (b) Spectral phase shift resulting from a 5% decrease in pump intensity, for these particular saturation and phase-matching conditions.

curves corresponds to a change in the integral in (7) caused by this 5% change in pump intensity, and is a measure for the pump-induced phase shift. The resulting change in the spectral phase is shown in Fig. 10(b). Note that the shape of this curve strongly depends on the spectral shape of the phase mismatch  $\Delta k$ , which can be expected from (7). In this example,  $\Delta k$  corresponds to the phase-mismatch curve from Fig. 3(b). For the spectrum shown in Fig. 3(b), such a spectral phase shift would correspond to a 3% broadening of a Fourier-limited pulse, while the resulting change in carrier-envelope phase is found to be below 150 mrad (1/40th of a cycle). Because the CEP results from an average over spectral components, it is less affected by the varying  $\Delta k$ -induced phase shifts than the individual spectral components. Even without intensity fluctuations, the spectral phase added through (7) needs to be taken into account in the stretcher-compressor design.

### VI. APPLICATIONS OF FEW-CYCLE OPCPA SYSTEMS

The use of high-intensity few-cycle pulses is particularly beneficial in laser-based electron acceleration. Few-cycle laser pulses enable acceleration in the so-called bubble regime [96], leading to relatively efficient acceleration with significantly relaxed pulse energy requirements compared to acceleration with longer pulses. This approach has already produced electron bunches with 25 MeV energy [97].

Another application of OPCPA is precision frequency measurements through Ramsey spectroscopy [98], [99]. This technique requires a pair of accurately phase-locked pulses with an interpulse time delay in the nanosecond range. The ability of OPCPA to amplify such closely spaced pulse pairs while maintaining their relative phase [95] is instrumental for this type of precision experiments. Combined with high-harmonic generation, this approach has recently led to a precision measurement of the 1s-5p transition in Helium at a wavelength of 51 nm, with an absolute frequency accuracy of 6 MHz [100].

An exciting development in laser science is the ability to produce coherent beams at ever shorter wavelengths through high-harmonic generation (HHG). Intense few-cycle pulses have been shown to improve the efficiency of HHG, making OPCPA systems useful candidates for the production of bright XUV and soft-X-ray beams. Significant progress has recently been made in this field by the demonstration of phase-matched HHG in the water-window spectral range [101], and even up to photon energies of 500 eV [102]. A key requirement is the use of longer driving wavelengths for HHG, for which OPCPA seems ideally suited.

Due to the young age of the field and the rapid progress being made, many more applications can be expected to appear in the near future. The designs of ultrahigh-intensity laser facilities, such as the extreme light infrastructure (ELI) and the petawatt field synthesizer, which should combine unprecedented peak intensities (in the petawatt to exawatt range) with few-cycle pulse duration, are based on OPCPA technology [103].

## VII. CONCLUSION

Research on few-cycle pulse generation is extremely active, and OPCPA technology has established itself in recent years as a powerful tool in this field. Significant progress has been made in recent years in pushing the limits in terms of peak power and pulse duration of OPCPA systems. The inherent phase stability of parametric amplification has enabled the development of CEP-stable OPCPA systems, which will be useful tools for many controlled light-field experiments and attosecond physics.

## REFERENCES

- [1] C. C. Wang and G. W. Racette, "Measurement of parametric gain accompanying optical difference frequency generation," *Appl. Phys. Lett.*, vol. 6, pp. 169–171, 1965.
- [2] S. E. Harris, M. K. Oshman, and R. L. Byer, "Observation of tunable optical parametric fluorescence," *Phys. Rev. Lett.*, vol. 18, pp. 732–734, 1967.
- [3] A. Baltuska, T. Fuji, and T. Kobayashi, "Visible pulse compression to 4 fs by optical parametric amplification and programmable dispersion control," *Opt. Lett.*, vol. 27, pp. 306–308, 2002.
- [4] J. Piel, M. Beutter, and E. Riedle, "20–50-fs pulses tunable across the near infrared from a blue-pumped noncollinear parametric amplifier," *Opt. Lett.*, vol. 25, pp. 180–182, 2000.
- [5] E. Riedle, M. Beutter, S. Lochbrunner, J. Piel, S. Schenkl, S. Spörlein, and W. Zinth, "Generation of 10 to 50 fs pulses tunable through all of the visible and the NIR," *Appl. Phys. B*, vol. 71, pp. 457–465, 2000.
- [6] G. Cerullo and S. De Silvestri, "Ultrafast optical parametric amplifiers," *Rev. Sci. Instrum.*, vol. 74, pp. 1–18, 2003.
- [7] D. Brida, G. Cirmi, C. Manzoni, P. Bonora, P. Villorresi, S. De Silvestri, and G. Cerullo, "Sub-two-cycle light pulses at 1.6  $\mu\text{m}$  from an optical parametric amplifier," *Opt. Lett.*, vol. 33, pp. 741–743, 2008.
- [8] C. Vozzi, F. Calegari, E. Benedetti, S. Gasilov, G. Sansone, G. Cerullo, M. Nisoli, S. De Silvestri, and S. Stagira, "Millijoule-level phase-stabilized few-optical-cycle infrared parametric source," *Opt. Lett.*, vol. 32, pp. 2957–2959, 2007.
- [9] D. Strickland and G. Mourou, "Compression of amplified chirped optical pulses," *Opt. Commun.*, vol. 56, pp. 219–221, 1985.
- [10] S. Backus, C. G. Durfee, M. M. Murnane, and H. C. Kapteyn, "High power ultrafast lasers," *Rev. Sci. Instrum.*, vol. 69, pp. 1207–1223, 1998.
- [11] A. Dubietis, G. Jonusauskas, and A. Piskarskas, "Powerful femtosecond pulse generation by chirped and stretched pulse parametric amplification in BBO crystal," *Opt. Commun.*, vol. 88, pp. 437–440, 1992.
- [12] I. N. Ross, P. Matousek, M. Towrie, A. J. Langley, and J. L. Collier, "The prospects for ultrashort pulse duration and ultrahigh intensity using optical parametric chirped pulse amplifiers," *Opt. Commun.*, vol. 144, pp. 125–133, 1997.
- [13] I. N. Ross, J. L. Collier, P. Matousek, C. N. Danson, D. Neely, R. M. Allott, D. A. Pepler, C. Hernandez-Gomez, and K. Osvay, "Generation of terawatt pulses by use of optical parametric chirped pulse amplification," *Appl. Opt.*, vol. 39, pp. 2422–2427, 2000.
- [14] S. Witte, R. T. Zinkstok, W. Hogervorst, and K. S. E. Eikema, "Generation of few-cycle terawatt light pulses using optical parametric chirped pulse amplification," *Opt. Express*, vol. 13, pp. 4903–4908, 2005.
- [15] D. Herrmann, L. Veisz, R. Tautz, F. Tavella, K. Schmid, V. Pervak, and F. Krausz, "Generation of sub-three-cycle, 16 TW light pulses by using noncollinear optical parametric chirped-pulse amplification," *Opt. Lett.*, vol. 34, pp. 2459–2461, 2009.
- [16] R. Butkus, R. Danielius, A. Dubietis, A. Piskarskas, and A. Stabinis, "Progress in chirped pulse optical parametric amplifiers," *Appl. Phys. B*, vol. 79, pp. 693–700, 2004.
- [17] A. Dubietis, R. Butkus, and A. Piskarskas, "Trends in chirped pulse optical parametric amplification," *IEEE J. Sel. Topics Quantum Electron.*, vol. 12, no. 2, pp. 163–172, Mar./Apr. 2006.
- [18] J. A. Armstrong, N. Bloembergen, J. Ducuing, and P. S. Pershan, "Interactions between light waves in a nonlinear dielectric," *Phys. Rev.*, vol. 127, pp. 1918–1939, 1962.
- [19] R. A. Baumgartner and R. L. Byer, "Optical parametric amplification," *IEEE J. Quantum Electron.*, vol. QE-15, no. 6, pp. 432–444, Jun. 1979.
- [20] R. A. Fischer and W. K. Bischel, "Numerical studies of the interplay between self-phase modulation and dispersion for intense plane-wave laser pulses," *J. Appl. Phys.*, vol. 46, pp. 4921–4934, 1975.
- [21] G. P. Agrawal, *Nonlinear Fiber Optics*, 2nd ed. San Francisco, CA: Academic Press, 1995.
- [22] I. N. Ross, P. Matousek, G. H. C. New, and K. Osvay, "Analysis and optimization of optical parametric chirped pulse amplification," *J. Opt. Soc. Amer. B*, vol. 19, pp. 2945–2956, 2002.
- [23] E. J. Grace, C. L. Tsangaris, and G. H. C. New, "Competing processes in optical parametric chirped pulse amplification," *Opt. Commun.*, vol. 261, pp. 225–230, 2006.
- [24] S. Witte, R. T. Zinkstok, W. Hogervorst, and K. S. E. Eikema, "Numerical simulations for performance optimization of a few-cycle terawatt NOPCPA system," *Appl. Phys. B*, vol. 87, pp. 677–684, 2007.
- [25] J. Moses, C. Manzoni, S.-W. Huang, G. Cerullo, and F. X. Kaertner, "Temporal optimization of ultrabroadband high-energy OPCPA," *Opt. Express*, vol. 17, pp. 5540–5555, 2009.
- [26] J. Zheng and H. Zacharias, "Non-collinear optical parametric chirped-pulse amplifier for few-cycle pulses," *Appl. Phys. B*, vol. 97, pp. 765–779, 2009.
- [27] V. Pyragaitė, A. Stabinis, R. Butkus, R. Antipenkov, and A. Varanavičius, "Parametric amplification of chirped optical pulses under pump depletion," *Opt. Commun.*, vol. 283, pp. 1144–1151, 2010.
- [28] O. Chalus, P. K. Bates, and J. Biegert, "Design and simulation of few-cycle optical parametric chirped pulse amplification at mid-IR wavelengths," *Opt. Express*, vol. 16, pp. 21 297–21 304, 2008.
- [29] C. Erny, L. Gallmann, and U. Keller, "High-repetition-rate femtosecond optical parametric chirped-pulse amplifier in the mid-infrared," *Appl. Phys. B*, vol. 96, pp. 257–269, 2009.
- [30] T. Wilhelm, J. Piel, and E. Riedle, "Sub-20-fs pulses tunable across the visible from a blue-pumped single-pass noncollinear parametric converter," *Opt. Lett.*, vol. 22, pp. 1494–1496, 1997.
- [31] G. M. Gale, M. Cavallari, T. J. Driscoll, and F. Hache, "Sub-20-fs tunable pulses in the visible from an 82-MHz optical parametric oscillator," *Opt. Lett.*, vol. 20, pp. 1562–1564, 1995.
- [32] P. Di Trapani, A. Andreoni, G. P. Banfi, C. Solcia, R. Danielius, A. Piskarskas, P. Foggi, M. Monguzzi, and C. Sozzi, "Group-velocity self-matching of femtosecond pulses in noncollinear parametric generation," *Phys. Rev. A*, vol. 51, pp. 3164–3168, 1995.
- [33] R. T. Zinkstok, S. Witte, W. Hogervorst, and K. S. E. Eikema, "High-power parametric amplification of 11.8-fs laser pulses with carrier-envelope phase control," *Opt. Lett.*, vol. 30, pp. 78–80, 2005.
- [34] S. Witte, R. T. Zinkstok, A. L. Wolf, W. Hogervorst, W. Ubachs, and K. S. E. Eikema, "A source of 2 terawatt, 2.7 cycle laser pulses based on noncollinear optical parametric chirped pulse amplification," *Opt. Express*, vol. 14, pp. 8168–8177, 2006.
- [35] N. Ishii, L. Turi, V. S. Yakovlev, T. Fuji, F. Krausz, A. Baltuska, R. Butkus, G. Veitas, V. Smilgevičius, R. Danielius, and A. Piskarskas, "Multimillijoule chirped parametric amplification of few-cycle pulses," *Opt. Lett.*, vol. 30, pp. 567–569, 2005.

- [36] F. Tavella, A. Marcinkevicius, and F. Krausz, "90 mJ parametric chirped pulse amplification of 10 fs pulses," *Opt. Express*, vol. 14, pp. 12 822–12 827, 2006.
- [37] J. Limpert, C. Agueraray, S. Montant, I. Manek-Höninger, S. Petit, D. Descamps, E. Cormier, and F. Salin, "Ultra-broad bandwidth parametric amplification at degeneracy," *Opt. Express*, vol. 13, pp. 7386–7392, 2005.
- [38] T. Fuji, N. Ishii, C. Y. Teisset, X. Gu, T. Metzger, A. Baltuska, N. Forget, D. Kaplan, A. Galvanauskas, and F. Krausz, "Parametric amplification of few-cycle carrier-envelope phase-stable pulses at 2.1  $\mu\text{m}$ ," *Opt. Lett.*, vol. 31, pp. 1103–1105, 2006.
- [39] J. Moses, S.-W. Huang, K.-H. Hong, O. D. Mücke, E. L. Falcão-Filho, A. Benedick, F. Ö. Ilday, A. Dergachev, J. A. Bolger, B. J. Eggleton, and F. X. Kärtner, "Highly stable ultrabroadband mid-IR optical parametric chirped-pulse amplifier optimized for superfluorescence suppression," *Opt. Lett.*, vol. 34, pp. 1639–1641, 2009.
- [40] N. Ishii, C. Y. Teisset, T. Fuji, S. Kohler, K. Schmid, L. Veisz, A. Baltuska, and F. Krausz, "Seeding of an eleven femtosecond optical parametric chirped pulse amplifier and its  $\text{Nd}^{3+}$  picosecond pump laser from a single broadband Ti: Sapphire oscillator," *IEEE J. Sel. Topics Quantum Electron.*, vol. 12, no. 2, pp. 173–180, Mar/Apr. 2006.
- [41] C. Y. Teisset, N. Ishii, T. Fuji, T. Metzger, S. Kohler, R. Holzwarth, A. Baltuska, A. Zheltikov, and F. Krausz, "Soliton-based pump-seed synchronization for few-cycle OPCPA," *Opt. Express*, vol. 13, pp. 6550–6557, 2005.
- [42] J. V. Rudd, R. J. Law, T. S. Luk, and S. M. Cameron, "High-power optical parametric chirped-pulse amplifier system with a 1.55  $\mu\text{m}$  signal and a 1.064  $\mu\text{m}$  pump," *Opt. Lett.*, vol. 30, pp. 1974–1976, 2005.
- [43] D. Kraemer, R. Hua, M. L. Cowan, K. Franjic, and R. J. D. Miller, "Ultrafast noncollinear optical parametric chirped pulse amplification in  $\text{KTiOAsO}_4$ ," *Opt. Lett.*, vol. 31, pp. 981–983, 2006.
- [44] L. J. Waxer, V. Bagnoud, I. A. Begishev, M. J. Guardalben, J. Puth, and J. D. Zuegel, "High-conversion-efficiency optical parametric chirped-pulse amplification system using spatiotemporally shaped pump pulses," *Opt. Lett.*, vol. 28, pp. 1245–1247, 2003.
- [45] J. A. Fülöp, Z. Major, B. Horvath, F. Tavella, A. Baltuska, and F. Krausz, "Shaping of picosecond pulses for pumping optical parametric amplification," *Appl. Phys. B*, vol. 87, pp. 79–84, 2007.
- [46] Y. Stepanenko and C. Radzewicz, "High-gain multipass noncollinear optical parametric chirped pulse amplifier," *Appl. Phys. Lett.*, vol. 86, 211120, 2005.
- [47] Y. Stepanenko and C. Radzewicz, "Multipass non-collinear optical parametric amplifier for femtosecond pulses," *Opt. Express*, vol. 14, pp. 779–785, 2006.
- [48] P. Wnuk, Y. Stepanenko, and C. Radzewicz, "Multi-terawatt chirped pulse optical parametric amplifier with a time-shear power amplification stage," *Opt. Express*, vol. 17, pp. 15 264–15 273, 2009.
- [49] F. Tavella, K. Schmid, N. Ishii, A. Marcinkevicius, L. Veisz, and F. Krausz, "High-dynamic range pulse-contrast measurements of a broadband optical parametric chirped-pulse amplifier," *Appl. Phys. B*, vol. 81, pp. 753–756, 2005.
- [50] V. Bagnoud, J. D. Zuegel, N. Forget, and C. Le Blanc, "High-dynamic-range temporal measurements of short pulses amplified by OPCPA," *Opt. Express*, vol. 15, pp. 5504–5511, 2007.
- [51] H. Kiriya, M. Mori, Y. Nakai, Y. Yamamoto, M. Tanoue, A. Akutsu, T. Shimomura, S. Kondo, S. Kanazawa, H. Daido, T. Kimura, and N. Miyanaga, "High-energy, high-contrast, multiterawatt laser pulses by optical parametric chirped-pulse amplification," *Opt. Lett.*, vol. 32, pp. 2315–2317, 2007.
- [52] N. Forget, A. Cotel, E. Brambrink, P. Audebert, C. Le Blanc, A. Jullien, O. Albert, and G. Chériaux, "Pump-noise transfer in optical parametric chirped-pulse amplification," *Opt. Lett.*, vol. 30, pp. 2921–2923, 2005.
- [53] I. N. Ross, G. H. C. New, and P. K. Bates, "Contrast limitation due to pump noise in an optical parametric chirped pulse amplification system," *Opt. Commun.*, vol. 273, pp. 510–514, 2007.
- [54] M. Siebold, M. Hornung, R. Boedefeld, S. Podleska, S. Klingebiel, C. Wandt, F. Krausz, S. Karsch, R. Uecker, A. Jochmann, J. Hein, and M. C. Kaluza, "Terawatt diode-pumped Yb: CaF<sub>2</sub> laser," *Opt. Lett.*, vol. 33, pp. 2770–2772, 2008.
- [55] J. Tümmler, R. Jung, H. Stiel, P. V. Nickles, and W. Sandner, "High-repetition-rate chirped-pulse-amplification thin-disk laser system with joule-level pulse energy," *Opt. Lett.*, vol. 34, pp. 1378–1380, 2009.
- [56] T. Metzger, A. Schwarz, C. Y. Teisset, D. Sutter, A. Killi, R. Kienberger, and F. Krausz, "High-repetition-rate picosecond pump laser based on a Yb:YAG disk amplifier for optical parametric amplification," *Opt. Lett.*, vol. 34, pp. 2123–2125, 2009.
- [57] K.-H. Hong, J. T. Gopinath, D. Rand, A. M. Siddiqui, S.-W. Huang, E. Li, B. J. Eggleton, J. D. Hybl, T. Y. Fan, and F. X. Kärtner, "High-energy, kHz-repetition-rate, ps cryogenic Yb:YAG chirped-pulse amplifier," *Opt. Lett.*, vol. 35, pp. 1752–1754, 2010.
- [58] D. Brida, C. Manzoni, G. Cirri, M. Marangoni, S. Bonora, P. Villorosi, S. D. Silvestri, and G. Cerullo, "Few-optical-cycle pulses tunable from the visible to the mid-infrared by optical parametric amplifiers," *J. Opt.*, vol. 12, p. 013001, 2010.
- [59] O. V. Chekhlov, J. L. Collier, I. N. Ross, P. K. Bates, M. Notley, C. Hernandez-Gomez, W. Shaikh, C. N. Danson, D. Neely, P. Matousek, S. Hancock, and L. Cardoso, "35 J broadband femtosecond optical parametric chirped pulse amplification system," *Opt. Lett.*, vol. 31, pp. 3665–3667, 2006.
- [60] V. V. Lozhkarev, G. I. Freidman, V. N. Ginzburg, E. V. Katin, E. A. Khazanov, A. V. Kirsanov, G. A. Luchinin, A. N. Mal'shakov, M. A. Martyanov, O. V. Palashov, A. K. Poteomkin, A. M. Sergeev, A. A. Shaykin, I. V. Yakovlev, S. G. Garanin, S. A. Sukharev, N. N. Rukavishnikov, A. V. Charukhchev, R. R. Gerke, and V. E. Yashin, "200 TW 45 fs laser based on optical parametric chirped pulse amplification," *Opt. Express*, vol. 14, pp. 446–454, 2006.
- [61] V. V. Lozhkarev, G. I. Freidman, V. N. Ginzburg, E. V. Katin, E. A. Khazanov, A. V. Kirsanov, G. A. Luchinin, A. N. Mal'shakov, M. A. Martyanov, O. V. Palashov, A. K. Poteomkin, A. M. Sergeev, A. A. Shaykin, and I. V. Yakovlev, "Compact 0.56 Petawatt laser system based on optical parametric chirped pulse amplification in  $\text{KD}^*\text{P}$  crystals," *Laser Phys. Lett.*, vol. 4, pp. 421–427, 2007.
- [62] I. Jovanovic, C. A. Ebberts, and C. P. J. Barty, "Hybrid chirped-pulse amplification," *Opt. Lett.*, vol. 27, pp. 1622–1624, 2002.
- [63] X. Zhou, H. Lee, T. Kanai, S. Adachi, and S. Watanabe, "An 11-fs, 5-kHz optical parametric/Ti:sapphire hybrid chirped pulse amplification system," *Appl. Phys. B*, vol. 89, pp. 559–563, 2007.
- [64] H. Kiriya, M. Mori, Y. Nakai, T. Shimomura, M. Tanoue, A. Akutsu, S. Kondo, S. Kanazawa, H. Okada, T. Motomura, H. Daido, T. Kimura, and T. Tajima, "High-contrast, high-intensity laser pulse generation using a nonlinear preamplifier in a Ti:sapphire laser system," *Opt. Lett.*, vol. 33, pp. 645–647, 2008.
- [65] H. Kiriya, M. Mori, Y. Nakai, T. Shimomura, H. Sasao, M. Tanoue, S. Kanazawa, D. Wakai, F. Sasao, H. Okada, I. Daito, M. Suzuki, S. Kondo, K. Kondo, A. Sugiyama, P. R. Bolton, A. Yokoyama, H. Daido, S. Kawanishi, T. Kimura, and T. Tajima, "High temporal and spatial quality petawatt-class Ti:sapphire chirped-pulse amplification laser system," *Opt. Lett.*, vol. 35, pp. 1497–1499, 2010.
- [66] A. Shirakawa, I. Sakane, M. Takasaka, and T. Kobayashi, "Sub-5-fs visible pulse generation by pulse-front-matched noncollinear optical parametric amplification," *Appl. Phys. Lett.*, vol. 74, pp. 2268–2270, 1999.
- [67] T. Kobayashi, A. Shirakawa, and T. Fuji, "Sub-5-fs transform-limited visible pulse source and its application to real-time spectroscopy," *IEEE J. Sel. Topics Quantum Electron.*, vol. 7, no. 4, pp. 525–538, Jul/Aug. 2001.
- [68] A. Baltuska and T. Kobayashi, "Adaptive shaping of two-cycle visible pulses using a flexible mirror," *Appl. Phys. B*, vol. 75, pp. 427–443, 2002.
- [69] S. Adachi, H. Ishii, T. Kanai, N. Ishii, A. Kosuge, and S. Watanabe, "1.5 mJ, 6.4 fs parametric chirped-pulse amplification system at 1 kHz," *Opt. Lett.*, vol. 32, pp. 2487–2489, 2007.
- [70] S. Adachi, N. Ishii, T. Kanai, A. Kosuge, J. Itatani, Y. Kobayashi, D. Yoshitomi, K. Torizuka, and S. Watanabe, "5-fs, multi-mJ, CEP-locked parametric chirped-pulse amplifier pumped by a 450-nm source at 1 kHz," *Opt. Express*, vol. 16, pp. 14 341–14 352, 2008.
- [71] D. Kraemer, M. L. Cowan, R. Hua, K. Franjic, and R. J. D. Miller, "High-power femtosecond infrared laser source based on noncollinear optical parametric chirped pulse amplification," *J. Opt. Soc. Amer. B*, vol. 24, pp. 813–818, 2007.
- [72] O. D. Mücke, S. Ališauskas, A. J. Verhoef, A. Pugžlys, A. Baltuska, V. Smilgevičius, J. Pocius, L. Giniūnas, R. Danielius, and N. Forget, "Self-compression of millijoule 1.5  $\mu\text{m}$  pulses," *Opt. Lett.*, vol. 34, pp. 2498–2500, 2009.
- [73] O. D. Mücke, D. Sidorov, P. Dombi, A. Pugžlys, S. Ališauskas, V. Smilgevičius, N. Forget, J. Posius, L. Giniūnas, R. Danielius, and A. Baltuska, "10-mJ optically synchronized CEP-stable chirped parametric amplifier at 1.5  $\mu\text{m}$ ," *Opt. Spectrosc.*, vol. 108, pp. 456–462, 2010.

- [74] F. Rotermund, C. Yoon, V. Petrov, F. Noack, S. Kurimura, N.-E. Yu, and K. Kitamura, "Application of periodically poled stoichiometric LiTaO<sub>3</sub> for efficient optical parametric chirped pulse amplification at 1 kHz," *Opt. Express*, vol. 12, pp. 6421–6427, 2004.
- [75] W. B. Cho, K. Kim, H. Lim, J. Lee, S. Kurimura, and F. Rotermund, "Multikilohertz optical parametric chirped pulse amplification in periodically poled stoichiometric LiTaO<sub>3</sub> at 1235 nm," *Opt. Lett.*, vol. 32, pp. 2828–2830, 2007.
- [76] X. Gu, G. Marcus, Y. Deng, T. Metzger, C. Teisset, N. Ishii, T. Fuji, A. Baltuska, R. Butkus, V. Pervak, H. Ishizuki, T. Taira, T. Kobayashi, R. Kienberger, and F. Krausz, "Generation of carrier-envelope-phase-stable 2-cycle 740- $\mu$ J pulses at 2.1- $\mu$ m carrier wavelength," *Opt. Express*, vol. 17, pp. 62–69, 2009.
- [77] O. Chalus, P. K. Bates, M. Smolarski, and J. Biegert, "Mid-IR short-pulse OPCPA with micro-Joule energy at 100 kHz," *Opt. Express*, vol. 17, pp. 3587–3594, 2009.
- [78] O. Chalus, A. Thai, P. K. Bates, and J. Biegert, "Six-cycle mid-infrared source with 3.8  $\mu$ J at 100 kHz," *Opt. Lett.*, vol. 35, pp. 3204–3206, 2010.
- [79] C. Erny, C. Heese, M. Haag, L. Gallmann, and U. Keller, "High-repetition-rate optical parametric chirped-pulse amplifier producing 1- $\mu$ J, sub-100-fs pulses in the mid-infrared," *Opt. Express*, vol. 17, pp. 1340–1345, 2009.
- [80] C. Heese, C. R. Phillips, L. Gallmann, M. M. Fejer, and U. Keller, "Ultrabroadband, highly flexible amplifier for ultrashort midinfrared laser pulses based on aperiodically poled Mg:LiNbO<sub>3</sub>," *Opt. Lett.*, vol. 35, pp. 2340–2342, 2010.
- [81] P. Wnuk, Y. Stepanenko, and C. Radzewicz, "High gain broadband amplification of ultraviolet pulses in optical parametric chirped pulse amplifier," *Opt. Express*, vol. 18, pp. 7911–7916, 2010.
- [82] G. Arisholm, J. Biegert, P. Schlup, C. P. Hauri, and U. Keller, "Ultrabroadband chirped-pulse optical parametric amplifier with angularly dispersed beams," *Opt. Express*, vol. 12, pp. 518–530, 2004.
- [83] L. Cardoso and G. Figueira, "Bandwidth increase by controlled angular dispersion of signal beam in optical parametric amplification," *Opt. Express*, vol. 12, pp. 3108–3113, 2004.
- [84] L. Cardoso, H. Pires, and G. Figueira, "Increased bandwidth optical parametric amplification of supercontinuum pulses with angular dispersion," *Opt. Lett.*, vol. 34, pp. 1369–1371, 2009.
- [85] H. Liu, W. Zhao, Y. Yang, H. Wang, Y. Wang, and G. Chen, "Matching of both group-velocity and pulse-front for ultrabroadband three-wave-mixing with noncollinear angularly dispersed geometry," *Appl. Phys. B*, vol. 82, pp. 585–594, 2006.
- [86] E. Zeromskis, A. Dubietis, G. Tamosauskas, and A. Piskarskas, "Gain bandwidth broadening of the continuum-seeded optical parametric amplifier by use of two pump beams," *Opt. Commun.*, vol. 203, pp. 435–440, 2002.
- [87] D. Herrmann, R. Tautz, F. Tavella, F. Krausz, and L. Veisz, "Investigation of two-beam-pumped noncollinear optical parametric chirped-pulse amplification for the generation of few-cycle light pulses," *Opt. Express*, vol. 18, pp. 4170–4183, 2010.
- [88] J. A. Fülöp, Z. Major, A. Henig, S. Kruber, R. Weingartner, T. Clausnitzer, E.-B. Kley, A. Tünnermann, V. Pervak, A. Apolonski, J. Osterhoff, R. Hörlein, F. Krausz, and S. Karsch, "Short-pulse optical parametric chirped-pulse amplification for the generation of high-power few-cycle pulses," *New J. Phys.*, vol. 9, 438, 2007.
- [89] Y. Tang, I. Ross, C. Hernandez-Gomez, G. New, I. Musgrave, O. Chekhlov, P. Matousek, and J. Collier, "Optical parametric chirped-pulse amplification source suitable for seeding high-energy systems," *Opt. Lett.*, vol. 33, pp. 2386–2388, 2008.
- [90] D. Herrmann, C. Homann, R. Tautz, M. Scharrer, P. S. J. Russell, F. Krausz, L. Veisz, and E. Riedle, "Approaching the full octave: non-collinear optical parametric chirped pulse amplification with two-color pumping," *Opt. Express*, vol. 18, pp. 18 752–18 762, 2010.
- [91] P. Baum, S. Lochbrunner, J. Piel, and E. Riedle, "Phase-coherent generation of tunable visible femtosecond pulses," *Opt. Lett.*, vol. 28, pp. 185–187, 2003.
- [92] A. Baltuska, T. Fuji, and T. Kobayashi, "Controlling the carrier-envelope phase of ultrashort light pulses with optical parametric amplifiers," *Phys. Rev. Lett.*, vol. 88, 133901, 2002.
- [93] C. P. Hauri, P. Schlup, G. Arisholm, J. Biegert, and U. Keller, "Phase-preserving chirped-pulse optical parametric amplification to 17.3 fs directly from a ti:sapphire oscillator," *Opt. Lett.*, vol. 29, pp. 1369–1371, 2004.
- [94] A. Renault, D. Z. Kandula, S. Witte, A. L. Wolf, R. T. Zinkstok, W. Hogervorst, and K. S. E. Eikema, "Phase stability of terawatt-class ultrabroadband parametric amplification," *Opt. Lett.*, vol. 32, pp. 2363–2365, 2007.
- [95] D. Z. Kandula, A. Renault, C. Gohle, A. L. Wolf, S. Witte, W. Hogervorst, W. Ubachs, and K. S. E. Eikema, "Ultrafast double-pulse parametric amplification for precision ramsey metrology," *Opt. Express*, vol. 16, pp. 7071–7082, 2008.
- [96] M. Geissler, J. Schreiber, and J. Meyer-ter-Vehn, "Bubble acceleration of electrons with few-cycle laser pulses," *New J. Phys.*, vol. 8, 186, 2006.
- [97] K. Schmid, L. Veisz, F. Tavella, S. Benavides, R. Tautz, D. Herrmann, A. Buck, B. Hidding, A. Marcinkevicius, U. Schramm, M. Geissler, J. Meyer-ter Vehn, D. Habs, and F. Krausz, "Few-cycle laser-driven electron acceleration," *Phys. Rev. Lett.*, vol. 102, 124801, 2009.
- [98] S. Witte, R. T. Zinkstok, W. Ubachs, W. Hogervorst, and K. S. E. Eikema, "Deep-ultraviolet quantum interference metrology with ultrashort laser pulses," *Science*, vol. 307, pp. 400–403, 2005.
- [99] A. Marian, M. C. Stowe, J. R. Lawall, D. Felinto, and J. Ye, "United time-frequency spectroscopy for dynamics and global structure," *Science*, vol. 306, pp. 2063–2068, 2004.
- [100] D. Z. Kandula, C. Gohle, T. J. Pinkert, W. Ubachs, and K. S. E. Eikema, "Extreme ultraviolet frequency comb metrology," *Phys. Rev. Lett.*, vol. 105, 063001, 2010.
- [101] T. Popmintchev, M.-C. Chen, A. Bahabad, M. Gerrity, P. Sidorenko, O. Cohen, I. P. Christov, M. M. Murnane, and H. C. Kapteyn, "Phase matching of high harmonic generation in the soft and hard X-ray regions of the spectrum," *Proc. Natl. Acad. Sci. USA*, vol. 106, pp. 10 516–10 521, 2009.
- [102] M.-C. Chen, P. Arpin, T. Popmintchev, M. Gerrity, B. Zhang, M. Seaberg, D. Popmintchev, M. M. Murnane, and H. C. Kapteyn, "Bright, coherent, ultrafast soft x-ray harmonics spanning the water window from a tabletop light source," *Phys. Rev. Lett.*, vol. 105, 173901, 2010.
- [103] Z. Major, S. A. Trushin, I. Ahmad, M. Siebold, C. Wandt, S. Klingebiel, T.-J. Wang, J. A. Fülöp, A. Henig, S. Kruber, R. Weingartner, A. Popp, J. Osterhoff, R. Hörlein, J. Hein, V. Pervak, A. Apolonski, F. Krausz, and S. Karsch, "Basic concepts and current status of the petawatt field synthesizer - a new approach to ultrahigh field generation," *Laser Rev.*, vol. 37, pp. 431–436, 2009.



**Stefan Witte** received the M.Sc. and Ph.D. degrees in physics from the VU University, Amsterdam, The Netherlands, in 2002 and 2007, respectively.

From 2007 to 2010, he was a Postdoctoral Researcher in the Biophysics Group, VU University, where he is currently a Research Associate at the Institute for Lasers, Life and Biophotonics. In 2010–2011, he was a Research Associate in the Kapteyn-Murnane group, JILA, University of Colorado, Boulder. His research interests include ultrafast optics, optical-parametric chirped-pulse amplification development, coherent X-ray generation and imaging, and biomedical microscopy.

Dr. Witte was the recipient of a Netherlands Organization for Scientific Research (NWO) VENI grant in 2009.



**Kjeld S. E. Eikema** received the M.Sc and Ph.D. degrees in physics from the VU University, Amsterdam, The Netherlands, in 1991 and 1996, respectively.

From 1996 to 2000, he was a Postdoctoral Fellow at the Max Planck Institute for Quantum Optics, Munich, Germany, in the group of Prof. T. W. Hänsch. In 2000, he started a group on ultrafast laser physics at the VU University, where he is currently an Associate Professor, and a Professor by special appointment at the Rijksuniversiteit Groningen and

KVI. His research interests include frequency comb lasers and applications, such as precision tests, OPCPA development and ultraintense lasers, coherent X-ray generation, and imaging applications.

Prof. Eikema was the recipient of a NWO VIDI grant. For his work on short-wavelength generation and applications, he received the European Physical Society Fresnel Prize 2003. In 2007, he obtained a NWO VICI grant for his research activities involving ultrafast phase-controlled pulses.